NASA RESEARCH ON THE AERODYNAMICS OF

JET VTOL ENGINE INSTALLATIONS

By Richard E. Kuhn and Marion O. McKinney, Jr.

NASA Langley Research Center
Langley Station, Hampton, Va.

Presented at the AGARD Specialist Meeting
on Aerodynamics of Power Plant Installation

Tullahoma, Tennessee
October 25-27, 1965

NATIONAL AERONAUTICS AND
SPACE ADMINISTRATION
WASHINGTON

L-4506

ABSTRACT

84998

This paper summarizes some of the more pertinent results of NASA investigations related to the aerodynamics of jet VTOL engine installations. It shows that there is a base loss in hovering due to suction forces creased on the underside of the fuselage by the entrainment of ambient air in the slipstream, and that the magnitude of this effect is related to the turbulence in the jet stream and its consequent rate of mixing with ambient air. It also shows that there are large lift losses and pitching moments due to jet-free-stream interference and that these characteristics can be significantly altered by proximity to the ground. And, finally, it shows that simple bellmouth inlets give good pressure recovery and low distortion for vertically mounted lift engines if the inlet lip radius is sufficiently large, but that such inlets are not suitable for windmill starting of the engines.

Author

SYMBOLS

A_j — jet nozzle area, ft^2

C_V — effective nozzle velocity coefficient $\left(\frac{\text{Effective exit velocity}}{\text{Ideal exit velocity}}\right.$ where effective exit velocity is equal to $\left. T/m \right)$

D — diameter of nozzle or inlet, ft

D_e — equivalent diameter - diameter of a single nozzle having the same area as the sum of the several nozzles of a multijet configuration, ft

ΔD_V — drag increment due to free-stream velocity, lb

h — height above ground, ft

ΔL_B — lift increment due to jet-induced base pressures, lb

ΔL_V — lift increment due to free-stream velocity, lb

l_V — rolling moment at velocity V, lb-ft

$l_{V=0}$ — rolling moment at zero velocity, lb-ft

m — mass flow, slugs/sec

ΔM_V — pitching-moment increment due to free-stream velocity, lb-ft

P_o — ambient air pressure, lb/ft^2

P_T — total pressure, lb/ft^2

P_{T_o} — free-stream total pressure, lb/ft^2

$\Delta P_{T,av}$ — average total pressure loss at the face of the engine, lb/ft^2

P_{max} — maximum total pressure at the face of the engine, lb/ft^2

P_{min} — minimum total pressure at the face of the engine, lb/ft^2

q — dynamic pressure, lb/ft^2

q_i — dynamic pressure in the inlet, lb/ft^2

q_N	dynamic pressure at jet nozzle, lb/ft^2
q_x	dynamic pressure at station x-distance downstream of nozzle, lb/ft^2
S	wing or base plate area, ft^2
T	thrust, lb, or temperature, ^oF
T_N	temperature at the nozzle, ^oF
V, V_o	free-stream velocity, ft/sec
V_i	velocity in inlet, ft/sec
V_j	velocity in jet, ft/sec
W_i	inlet airflow, lb/sec
x	distance downstream of nozzle, ft
α	angle of attack, deg
β	angle of sideslip, deg
δ_a	aileron deflection, downward deflection is positive, deg
ρ_o	air density in free stream, $slugs/ft^3$
ρ_j	air density in jet, $slugs/ft^3$

NASA RESEARCH ON THE AERODYNAMICS OF

JET VTOL ENGINE INSTALLATIONS

By Richard E. Kuhn* and Marion O. McKinney, Jr.*

1. INTRODUCTION

The rated thrust of a jet engine, whether for a conventional aircraft or for a VTOL aircraft, is based on its test-stand performance with a bell-mouth inlet and the design nozzle for the engine. The actual performance of the engine in the airplane is degraded from this test-stand rating by various installation losses. In the case of jet VTOL aircraft where the engines must support the aircraft in hovering, the gross weight of the aircraft is directly reduced by these losses. There are several sources of lift or thrust loss, each of which are only a few percent of the rated thrust. However, an accurate knowledge of each is required to make realistic estimates of the expected aircraft performance. An error of as little as 3 percent in the total lifting capacity in hovering would mean a reduction of 3 percent in gross weight and, in turn, a reduction of over 10 percent in the fuel that could be carried, and, therefore, a large reduction in range from the design value.

This paper is not intended to cover all aspects of VTOL engine installation. Only some of the more interesting results of NASA investigations in the following areas are included:

(1) Exhaust nozzle losses

(2) Base losses in hovering out of ground effect

(3) Jet-free-stream induced lift loss and moment in transition in and out of ground effect

---

*Aerospace Engineer, Langley Research Center, Langley Station, Hampton, Va.

(4) Jet-free-stream interference effects on reaction control effectiveness

(5) Losses in inlet total pressure

The aerodynamic lift loss (suck down) in ground effect in hovering is another important loss and has been the subject of numerous investigations in the past, but it will be touched on only incidentally here.

The material presented herein is obtained from wind-tunnel and static-force-test models. The NASA flight experience with the Bell X-14A aircraft is being presented in another paper (ref. 1) at this same meeting.

2. NOZZLE AND BASE LOSSES IN HOVERING

2.1. Jet-Induced Base Loss

Basic problem.- When lifting engines are installed in an aircraft to exhaust vertically through the bottom of the fuselage or wing, a base loss which depends on several factors is encountered. This loss, as indicated by the sketch at the top of figure 1, arises from the entrainment action of the jet which induces suction pressures on the surface surrounding the jet exit. The lift loss created by these suction pressures for various arrangements of multiple jets was the subject of the investigation reported in reference 2. In this investigation some problems in properly simulating the jet flow were encountered.

Effect of model plenum chamber configuration.- It was realized at the beginning of the investigation that the rectangular plenum chamber, which was designed to fit inside the fuselage for the multiple jet investigation, was much smaller than would be desired. The first part of the investigation therefore was to obtain a comparison of the loads induced on a circular plate by a single nozzle from the rectangular plenum chamber for comparison with an identical plate-nozzle configuration on the more ideal circular plenum chamber. As shown in figure 1 the loads induced on the circular plate mounted on the original rectangular plenum were four to five times as large as those induced on the same size plate on the circular plenum chamber with a clean nozzle. Surveys of the exit flow from the rectangular plenum indicated a distorted velocity distribution with a loss at the center, whereas the flow from the circular plenum chamber had a flat distribution. Also it was obvious that the flow from the rectangular plenum chamber was extremely rough and it was suspected that this extreme turbulence of the flow was causing the higher induced loads. Two steps were taken in an attempt to check this hypothesis. The rectangular plenum chamber was modified by installation of some fairings and a redistribution of the orifices feeding the air into the chamber to improve the quality of the flow. Secondly, a strut was installed about 1 diameter upstream of the nozzle on the circular plenum chamber to produce a roughened flow. This also produced a much greater distortion of the velocity distribution than was present on the original rectangular plenum chamber. As shown by the lift-loss curves at the top of figure 2, these changes increased the lift loss for the cylindrical plenum chamber and greatly reduced the losses for the rectangular plenum chamber. These changes in the lift losses did not correlate with the exit velocity distribution.

The lift losses were found to correlate with the rate of decay of the jet with distance downstream from the exit as shown by the curves at the bottom of figure 2. These curves present the ratio of the peak of the dynamic pressure distribution at a distance x downstream of the nozzle divided by the dynamic pressure at the nozzle as a function of distance from the nozzle in nozzle diameters. As will be noted, the original rectangular plenum chamber exhibited the most rapid decay of dynamic pressure and produced the highest lift losses. The original circular plenum chamber with smooth flow had the lowest decay rate and the lowest lift losses. The modified rectangular plenum chamber and the circular chamber with the roughened flow had similar lift losses and similar decay curves.

The correlation between the rate of decay of the jet and the base losses induced by the jet is to be expected; both the base loss and the jet decay are caused by the action of the jet in entraining air and both should be proportional to the rate of entrainment. This correlation has also been found to hold for the multiple-jet configurations as shown in figure 3. These data were obtained with the modified rectangular plenum chamber. Here the decay curves are presented as a function of distance in terms of equivalent jet diameters where D_e represents the diameter of a single jet which would contain all of the area of the multiple jets. An empirical correlation of the base loss with the rate of decay of the jet was developed in reference 2 which produced the following expression:

$$\frac{\Delta L_B}{T} = -0.09\sqrt{S/A_j}\sqrt{\left(\frac{\partial \frac{q_x}{q_N}}{\partial \frac{x}{D_e}}\right)_{max} \Bigg/ \left(\frac{x}{D_e}\right)_i}$$

where $\left(\frac{\partial \frac{q_x}{q_N}}{\partial \frac{x}{D_e}}\right)_{max}$ is the maximum rate of decay of the dynamic pressure in the jet and $\left(\frac{x}{D_e}\right)_i$ is the distance downstream at which this maximum decay rate occurs, that is, the inflection point of the decay curve. Additional data on the effect of wing height on nozzle projection below the fuselage are given in reference 2.

Small-scale—large-scale comparison.- The preceding base-loss data were obtained using small cold jets with an equivalent diameter of 2.25 inches. In view of the importance of the quality of the flow in the jet established in this study a second investigation (ref. 4) was undertaken using a full-scale J85 engine. The engine was equipped with two alternate tail pipes; one for a single-jet investigation and one with special exhaust ducting to produce a four-jet configuration. The investigations were run with three different sizes of rectangular plates to produce three different ratios of plate area to jet area. The comparison of these real engine data, shown by the darkened symbols in figure 3, with the model results indicates good agreement.

The correlation between the base loss and the rate of decay of the jet as presented above indicates a need for information on the decay rate for actual jet engines. Decay curves for only two full-scale jet engines could be found (refs. 4 and 5) and these are compared with the decay curves for the model jets used in the previous investigation as shown in figure 4. These limited full-scale data indicate that these engines at least are only slightly better than the modified plenum chamber configuration of the small-scale investigation and not as good as the circular plenum chamber where special attention was directed toward achieving a good quality jet. It is doubtful, however, that all jet engines will have decay curves similar to the two shown here. This is particularly true of lift engines which may use annular nozzles to decrease their length or other special nozzles to promote a rapid decay or to facilitate vectoring of the flow. It appears highly desirable to determine the decay curves for the various engines and nozzles that may be used in a jet VTOL aircraft.

The importance of the jet decay rate on other interference problems such as the suck down within ground effect in hovering and the jet-free-stream interference effects induced in transition flight have not been determined. It appears logical, however, that there should be some effects and it would appear desirable in the future to determine the decay rate of the jets used in any model investigations.

2.2. Exhaust Velocity Suppression

One of the problems that may face jet VTOL aircraft is that of the potential erosion of the ground by the jet blast. An investigation of the potential of various nozzle configurations for relieving this problem by promoting rapid decay of jet velocity with distance downstream of the nozzle is reported in references 6 and 7. Decay curves for three of the nozzles investigated are shown in figure 5. All three of the nozzles are convergent but the slot nozzles have one important feature which does not show clearly in the illustration. They have a 5° divergent angle between the small sides at the end of each slot. Decay curves were measured for all of the nozzles at two jet temperatures - 70° F and 1200° F. As can be seen in figure 5, a rapid decay can be obtained by using a multiple element nozzle arrangement and the temperature of the jet air does not have an appreciable effect on the decay rate except for the circular nozzle.

2.3. Nozzle Losses

Nozzle thrust losses and temperature decay rates as well as dynamic pressure decay rates were measured for a circular nozzle, a 12-segment nozzle, a single-slot nozzle, and nine multiple-slot nozzle configurations with variations in slot aspect ratio, slot spacing, and divergence angles of the small walls of each slot. The thrust loss (difference between ideal thrust and measured thrust) on these nozzles is plotted in figure 6 as a function of the dynamic pressure reduction Δq and the jet temperature reduction ΔT at a distance of 3 diameters from the nozzle. The thrust loss presented is the difference between the ideal thrust and the measured thrust and includes both internal and external losses. The boundaries shown are not fundamental but represent the envelope of the best performance obtained from the 12 nozzles.

In view of the importance of the decay curves to the base loss, as discussed previously, some of the nozzles were tested both alone and with a large plate surrounding the nozzle to represent the lower surface of a wing or fuselage. As shown in figure 6, the installation of this fuselage appreciably increased the thrust losses. (The thrust loss shown for the with-fuselage case includes the base-loss forces on the fuselage.) The increment between the nozzle-alone and with-fuselage curve shown in figure 6, however, is appreciably less than would be estimated from the decay curves and the base-loss equations shown above. This discrepancy indicates the importance and problem of proper application of nozzle and base-loss data as discussed below.

2.4. Superposition of Base Loss and Nozzle Loss

It was noted in reference 7 that high suction pressures were generated on the surfaces between the slots of the multiple-slot nozzle as would be expected. These and similar pressures induced on the sloping exterior sides of the nozzles are induced by the entrainment action of the jet and represent a "base loss" that is contained in the nozzle-alone data. That is, as indicated in figure 7, the nozzle-alone data are a combination of internal and external losses. In order to properly apply the base-loss data of reference 2 and the nozzle-loss data such as that obtained from reference 7, it is necessary to determine how much of this nozzle loss is external loss; or, stated another way, to determine how much of the base loss is already included in the nozzle-loss data. The investigation of reference 7 was not set up to determine this breakdown and the breakdown cannot be made with accuracy; however, it appears that even the circular-nozzle-loss data contain some external loss and that anywhere from 1/3 to 1/2 of the nozzle losses could be external losses.

If the slots are far enough apart (as with a single slot per engine on a multiengine configuration) ground proximity can give favorable pressures between the slots as indicated below. The spacing of multiple slots on a single engine nozzle, as investigated in reference 7, is too close to experience this favorable effect, however.

3. INTERFERENCE EFFECTS IN TRANSITION

The loss in lift and the nose-up pitching moment created by suction pressures induced beside and behind the jets by interference with the free-stream flow in transition flight have been the subject of numerous investigations by NASA and many other organizations (see refs. 9 and 10, for instance). Most of these investigations have been made out of ground effect and with only the exit flow simulated. Two recent studies have been made to investigate the effects of ground proximity and to investigate the possibility of mutual interference effects between the inlet and exit flows.

3.1. Ground Effects on Jet Interference

The effects of ground proximity on the loss in lift and nose-up pitching moment induced on a wing-body combination for six different arrangements of vertical jets were investigated in reference 10. Data for three of these configurations are presented in figure 8 to show the comparison of the induced effects out of ground effect with those obtained at a height of 1 effective diameter. The data shown here represent only the jet-induced forces due to free-stream velocity and due to ground proximity. The direct thrust of the jet, the base loss, and the aerodynamic forces corresponding to the power-off condition have been subtracted from the data to leave only the interference lifts and moments due to velocity and ground. The data are presented as a function of the effective velocity ratio, as suggested in reference 11, which is the square root of the ratio of free stream to jet momentum per unit area, and which takes into account the difference in density resulting from differences in jet temperature.

The data of figure 8 indicate some significant effects of the ground on the interference effects. For the single-jet case a very large suck down was experienced in hovering (effective velocity ratio of 0) in ground effect, but the additional lift loss due to velocity was only slightly affected by the ground. The induced pitching moment due to velocity, however, was greatly reduced indicating that the suction pressures behind the jet were probably reduced by ground effect and those beside the jet were increased. The four-jet case, as would be expected, shows considerably less suck down due to ground effect at zero effective velocity ratio and shows a marked reduction in both the lift and pitching moment induced by forward velocity thus indicating a general reduction in the induced suction pressures. The two-slot configurations which had a favorable ground effect at zero speed experienced a slight increase in interference effects due to forward velocity. In general, the data of reference 10 and figure 8 indicate that the effects of ground proximity on the jet-free-stream effects are highly configuration dependent and that no general conclusions can be drawn at this time.

3.2. Mutual Inlet-Exit Interference Effects

The question of the applicability of the principle of superposition to the problems of exit interference effects and inlet interference effects in combination has frequently been raised; that is, can the exit effects be measured on one rig and the inlet effects on another and the results simply added to determine the characteristics of the total configuration. An investigation was recently undertaken to investigate this problem for a lift-engine-type installation. The results shown in figure 9 illustrate the data obtained for the simulation of a single engine in a body. The exit thrust to inlet weight-flow condition simulated corresponded to a lift fan engine with a bypass ratio of about 2. The model was set up so that the air drawn into the inlet could be pumped off independent of the exit. The air for the exit was brought into the model separately through high-pressure tubing, thus the inlet and the exit could be run separately or simultaneously.

The data shown in figure 9 indicate that within the accuracy of the data there are little or no mutual interference effects. The pitching moment due to the inlet corresponds to the inlet drag at a distance of a little over 1 inlet diameter above the upper surface of the body. The sum of this inlet moment and the exit interference moment is almost identical to the measured data with both the inlet and the exit operating simultaneously. The drag increment due to the inlet operating alone is exactly equal to the calculated inlet momentum drag. The exit drag appears to be due to positive pressures induced on the curved surface ahead of the exit. The sum of the drag increment measured on the inlet and exit separately is slightly less than the drag measured with the inlet and exit operating simultaneously. The difference, however, is the same as the order of the accuracy of the drag data; so, in general, figure 9 indicates negligible mutual interference between the inlet and exit flows.

There are a wide variety of configurations on which the possibility of mutual interference effects between the inlet and exit flows might be encountered. The present investigation covers only one, a lift engine with a fairly small inlet mass flow installed in a rather large body. Similar investigations involving other configurations with much larger inlet mass flow and with the inlet and exit in much closer proximity than was possible in the present simple model will be required before it can be stated conclusively that there are no inlet-exit mutual interference effects to be concerned with.

3.3 Interference Effects on Reaction Controls in Transition

The losses in lift induced by the jet-free-stream interference effects discussed in the previous section have been found to be a function of the ratio of the model planform area to jet area. This fact has suggested that the effectiveness of reaction-control jets such as the roll-control jets near the wing tip may suffer significant losses in effectiveness in transition in view of the very high ratios of wing area to jet area involved in such installations. A wind-tunnel investigation of this problem was undertaken in which the roll-control jets were operated at a pressure ratio of 6. Results are shown in figures 10 and 11 in terms of the ratio of roll control at a given velocity to the roll control produced by the reaction jet in hovering as a function of full-scale aircraft velocity. The data are shown for the case where two jets in tandem were used to provide the necessary reaction control moment. The expected reduction in control effectiveness with forward speed was found for the case of 0° sideslip angle. The loss in effectiveness was greatly increased at a positive sideslip deflection and greatly reduced, and in fact converted to a slight increase in effectiveness, at a negative sideslip angle. These effects of sideslip angle are much larger than anticipated and are not presently understood. The favorable effects of the negative sideslip case give hope that when the reasons for these larger effects are understood configurations may be designed which will minimize or eliminate the loss in effectiveness. The significance of the loss in effectiveness for the worst encountered sideslip angle of 30°, is shown in the plot at the right of figure 10 which shows that 15° deflection of each aileron is required to compensate for this loss in effectiveness. Thus, a large part of the normal aileron controls is used for this purpose and the total roll control for a typical airplane in transition from hovering to normal flight may not be much greater than that in hovering whereas the roll-control requirements due to dihedral effect and rolling moments induced by the main jets in sideslip in this range may be much greater than the hovering-control requirements.

Two attempts were made to reduce the adverse interference effects on the roll control in this investigation. These were (1) to move the roll-control jets from the leading edge to the trailing edge of the wing and (2) to move them to the wing tip (which was accomplished by removing the parts of the wing panel outboard of the jets). As can be seen in figure 11, these two modifications eliminated most of the adverse interference effects for the condition of zero sideslip. The increments produced by these modifications were about the same for the 30° sideslip case but large losses in effectiveness still remain.

4. INLET CHARACTERISTICS

4.1. Inlet Pressure Recovery

An investigation of the inlet-pressure-recovery characteristics of pod-mounted lift engines has been undertaken by the NASA Ames Research Center using full-scale engines. The model used five J85 engines mounted in a pod supported from a stub wing as shown by the photograph of figure 12. No difficulties attributable to the inlets were encountered in using the engines during the investigation. Both simple bellmouth inlets, as shown in figure 12, and inlets with scoop-type doors, as shown in figure 13, were used.

Some of the results of the investigation are shown in figure 14. This figure shows inlet distortion or pressure loss for the pod with bellmouth inlets for a speed of 150 knots, which is intended to represent approximately the maximum speed at which the lift engines would have to be operated. The total pressure recovery is given by $\frac{\Delta P_{T,av}}{q_i}$, and the distortion, by the parameter $\frac{P_{T,max} - P_{T,min}}{P_{T_o}}$ which indicates the maximum total-pressure difference across the face of the engine as a fraction of the free-stream total pressure. Three points should be noted from these data. First, at full engine thrust the inlet pressure losses are small and the distortion is low. Second, that the losses and distortion are greatest for inlets 2 and 3 which are near the high suction region at the leading edge of the wing. The effect of this proximity of the inlet to the leading edge of the wing is greatest at high angles of attack where the leading-edge suction forces are the greatest. And, finally, the distortion and total pressure loss are most severe for the idle thrust case, but no difficulties were experienced with the J85 engines under these inlet conditions. The amount and type of distortion that can be tolerated vary considerably from one engine to another, and whether or not these values would be acceptable with other engines is not known. Additional correlation and analysis of available inlet data are needed to arrive at a distortion criterion that can be used as a guide in the design of both inlets and engines. In the mean time the value of 8- to 10-percent distortion experienced here might be used as a tentative guide.

Scoop inlets such as those shown in figure 13 were found to be no better than the simple bellmouth inlets with regard to flow distortion. In fact they had to be very carefully tailored to avoid having greater distortion than the simple bellmouth inlets.

For simple bellmouth inlets the radius of the upstream lip of the inlet is a critical design factor. If the inlet lip radius is too small, the flow will break away from the lip and give large distortions and pressure losses. Some data showing the effect of lip radius on pressure losses are given in figure 15. At the left in the figure is shown data on inlet total pressure loss (related to free-stream dynamic pressure) as a function of the inlet velocity ratio (free-stream velocity/ velocity at the face of the engine). These data are from a number of different sources, references 12 and 13 and unpublished data, and are also for both small-scale models and full-scale engine installations. The data show that as the velocity ratio increases the losses rise sharply, evidently as a result of inlet lip separation.

The plot at the right in figure 15 is a crossplot of the data at the left showing the inlet lip radius required to keep the inlet total-pressure losses down to an arbitrary 20 percent of the inlet dynamic pressure. This plot shows a rough correlation of velocity ratio with inlet radius, and also shows somewhat better performance at model scale. This latter point is surprising because previous experience with ducted propeller configurations (ref. 14) had indicated premature lip separation at small scale on the basis of force-test data. There are several factors that could account for the apparently better performance of the model inlets indicated by figure 15. In the case of the configuration of reference 13, where a direct-model—full-scale comparison was attempted, the survey plane location of the full-scale configuration could not be duplicated on the model because of the greater thickness of the model fan (ref. 15). Thus the survey was closer to the inlet on the model than on the full-scale article; and, as pointed out in reference 12, this would reduce the inlet losses thus determined. Also, the effect of the fan load distribution is unknown, but may be significant. The full-scale fan had a reasonably uniform radial distribution of load as compared to the model which was highly loaded toward the blade tips. The greater effectiveness of the tip sections of the model fan, as compared to the root sections which experienced some reversed flow, would tend to reduce the tendency for the flow to separate from the walls of the duct. Also all the inlets were vertical except those on the Ames 5-engine pod where the inlets were canted 10° ahead of vertical. Irrespective of these model—full-scale differences, the data of figure 15 emphasize the importance of providing adequate inlet lip radius to delay flow separation within the range of velocity ratios expected for the airplane.

4.2. Effect of Inlet on Engine Windmilling

Another characteristic that was investigated in the Ames tests with the lift-engine pod was engine windmilling with various inlets and at various angles of attack. Some of the data from the investigation are shown in figure 16. This figure shows plots of windmilling rpm (in percent rated engine rpm) as a function of angle of attack for the simple bellmouth inlets (with a deflector ahead of the exit of engine No. 1) and for scoop inlets. The data show that the simple bellmouth inlets were quite unsatisfactory from the standpoint of engine windmilling with a view toward windmill starting. Engine 4 would hardly windmill at all, and engine 3 windmilled in the wrong direction. On the other hand, the engines windmilled fairly well with the scoop inlets. It should be noted that, for either type of inlet, the windmilling rate for engine 3 dropped off markedly as angle of attack was increased. These characteristics probably resulted from the low-pressure field on the top of the wing near this inlet.

It was also observed during the tests that starting the engines with electric starters at 150 knots and $\alpha = 8^{\circ}$ was no problem with either type of inlet.

5. CONCLUDING REMARKS

This paper has summarized some of the more pertinent results of some recent NASA investigations related to the aerodynamics of jet VTOL engine installations. In many cases these are continuing programs and final conclusions cannot be stated at this point. The most pertinent conclusions from the present summary appear to be the following:

Jet-induced base loss in hovering.- The jet-induced base loss encountered in hovering out-of-ground effect is a function of the ratio of total configuration planform area to jet area and of the rate of decay of the jets. An accurate prediction of the base losses for a given configuration requires that the decay curves for full-scale engines, with the nozzles to be used in the aircraft installed, be known. Also, care must be exercised in applying base-loss increments and nozzle-thrust increments, to see that the external part of the nozzle loss is not accounted for twice in predicting the total system performance.

Interference effects in transition.- The jet-free-stream interference effects can cause large losses in lift and large pitching moments in the transition conditions. These effects can be altered significantly by proximity to the ground; but, the manner in which these increments are altered is highly configuration dependent. Similarly significant losses in roll control from reaction jets near the wing tips can be encountered at high transition speeds, particularly under high sideslip conditions. The decrease in effectiveness can be reduced by placing the control jets as close to the trailing edge and as close to the wing tip as possible. The mutual inlet-exit interference effects in transition for lift-engine configurations appear to be negligible - on the basis of very limited tests.

Inlet characteristics.- Simple bellmouth inlets of adequate lip radius (about one-half the inlet throat diameter) give reasonably high-pressure recoveries and low flow distortion throughout the transition range for lift engines. Scoop-type inlets have to be carefully tailored to give as low distortion as the bellmouth inlets. Bellmouth inlets, even with a deflector ahead of the engine exits, do not provide adequate engine windmilling characteristics for windmill starting - particularly at high angles of attack. Scoop inlets, however, can provide satisfactory windmilling characteristics.

REFERENCES

1. Rolls, L. Stewart: Jet VTOL Power Plant Experience During Flight Test of X-14A VTOL Research Vehicle. AGARD Specialists Meeting, Arnold Air Force Station, Tennessee, October 25-27, 1965.
2. Gentry, Carl L., and Margason, Richard J.: Jet-Induced Losses on VTOL Configurations Hovering In and Out of Ground Effect. NASA Proposed Technical Note, 1965.
3. Wygnanski, I.: The Flow Induced by Two-Dimensional and Axisymmetric Turbulent Jets Issuing Normally to an Infinite Plane Surface. Report No. 63-12. McGill University, Montreal, Canada.
4. McLemore, Huel C.: Investigation to Determine the Static Jet Induced Base Loss of a Turbojet Engine VTOL Configuration. NASA Proposed Technical Note, 1965.
5. Fleming, William A.: Characteristics of a Hot Jet Discharge From a Jet-Propulsion Engine. NACA RM No. E6L27a, 1946.
6. Higgins, C. C., and Wainwright, T. W.: Dynamic Pressure and Thrust Characteristics of Cold Jets Discharging from Several Exhaust Nozzles Designed for VTOL Downwash Suppression. NASA TN D-2263, 1964.
7. Higgins, C. C., Kelly, D. P., and Wainwright, T. W.: Exhaust Jet Wake and Thrust Characteristics of Several Nozzles Designed for VTOL Downwash Suppression - Tests In and Out of Ground Effect With 70° F and 1200° F Nozzle Discharge Temperatures. NASA Proposed Contractor Report, 1965.
8. Vogler, Raymond D.: Interference Effects of Single and Multiple Round or Slotted Jets on a VTOL Model in Transition. NASA TN D-2380, 1964.
9. Williams, John: Aerodynamic Interference Effect of the Jet-Lift Schemes for V/STOL Aircraft. AGARD Specialists Meeting, Arnold Air Force Station, Tennessee, October 25-27, 1965.

10. Vogler, Raymond D.: Ground Effects on a Multiple-Jet VTOL Model at Transition Speeds Over Stationary and Moving Ground Planes. NASA Proposed Technical Note, 1965.

11. Williams, John, and Butler, Sidney, F. J.: Further Developments in Low-Speed Wind-Tunnel Techniques for V/STOL and High-Lift Model Testing. RAE Tech. Note No. Aero. 2944, January 1964.

12. Tyson, B. I.: Tests of Air Inlets for Jet Lift Engines. Society of Automotive Engineers, preprint 860B, April 27-30, 1964.

13. Aoyagi, Kiyoshi, Hickey, David H., and deSavigny, Richard A.: Aerodynamic Characteristics of a Large-Scale Model With a High Disk-Loading Lifting Fan Mounted in the Fuselage. NASA TN D-775, 1961.

14. Grunwald, Kalman J., and Goodson, Kenneth W.: Division of Aerodynamic Loads on a Semispan Tilting-Ducted-Propeller Model in Hovering and Transition Flight. NASA TN D-1257, 1962.

15. Davenport, Edwin E., and Kuhn, Richard E.: Wind-Tunnel-Wall Effects and Scale Effects on a VTOL Configuration With a Fan Mounted in the Fuselage. NASA TN D-2560, 1965.

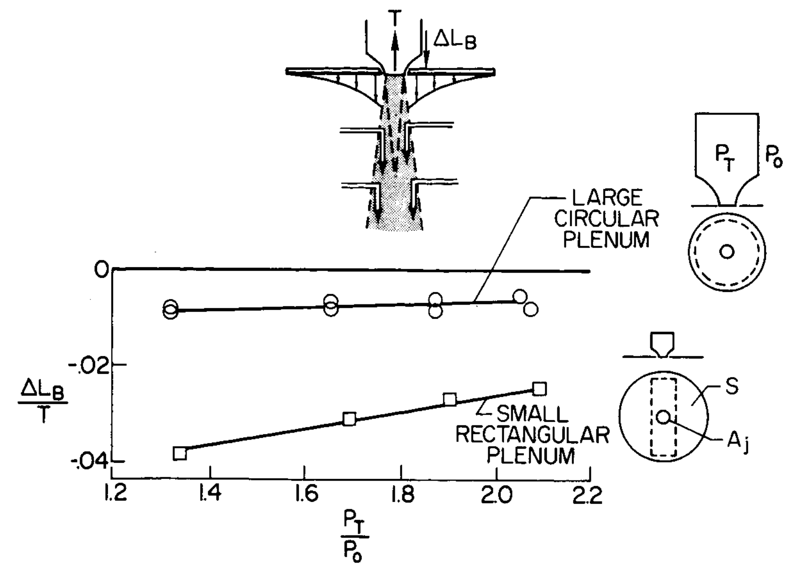

Figure 1.- Effect of plenum chamber configuration on base loss. $S/A_j = 69.5$.

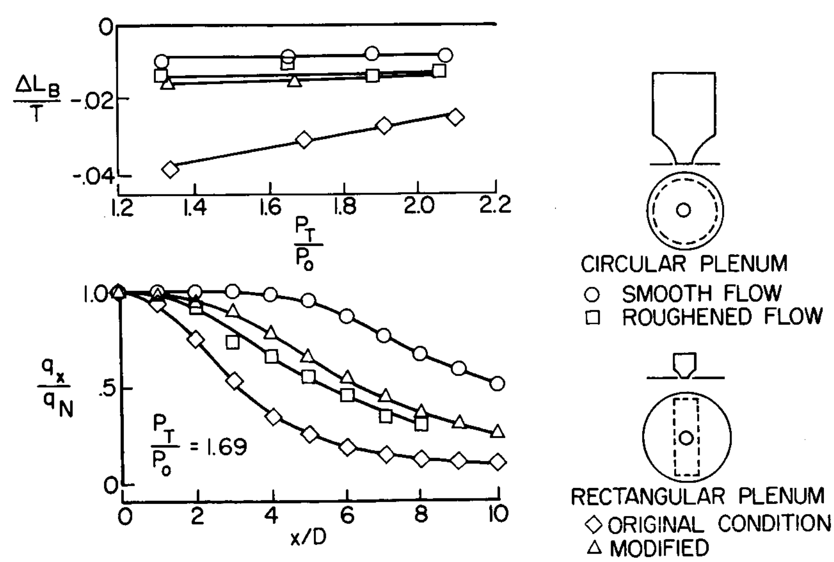

Figure 2.- Correlation of base loss with jet decay.

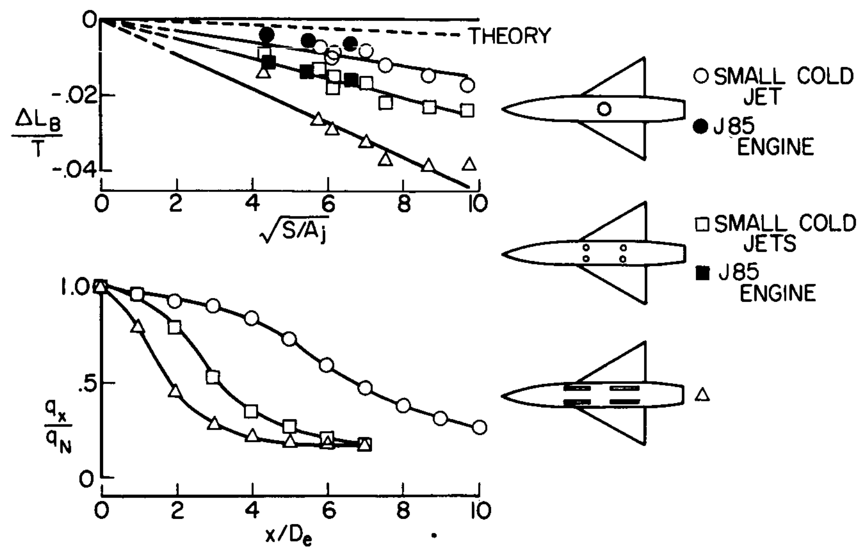

Figure 3.- Effect of jet arrangement on base loss and jet decay.

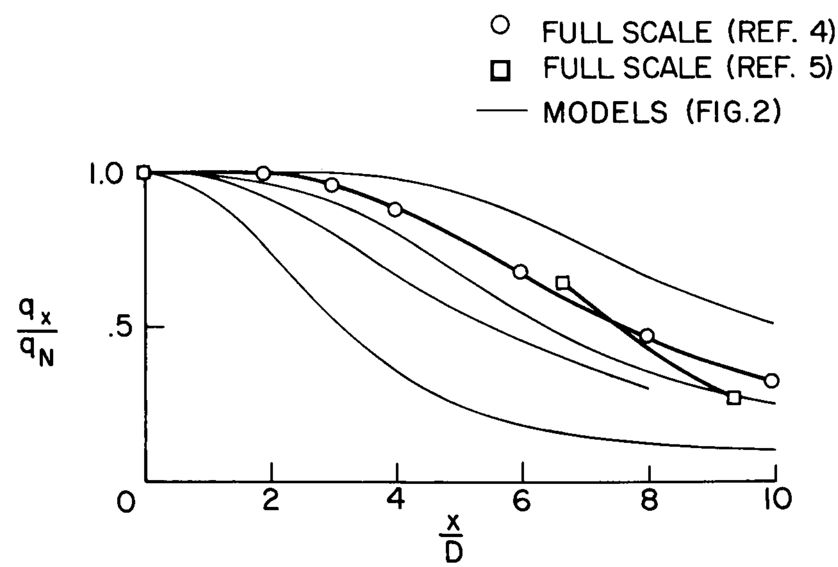

Figure 4.- Comparison of model jet and full-scale-engine jet decay.

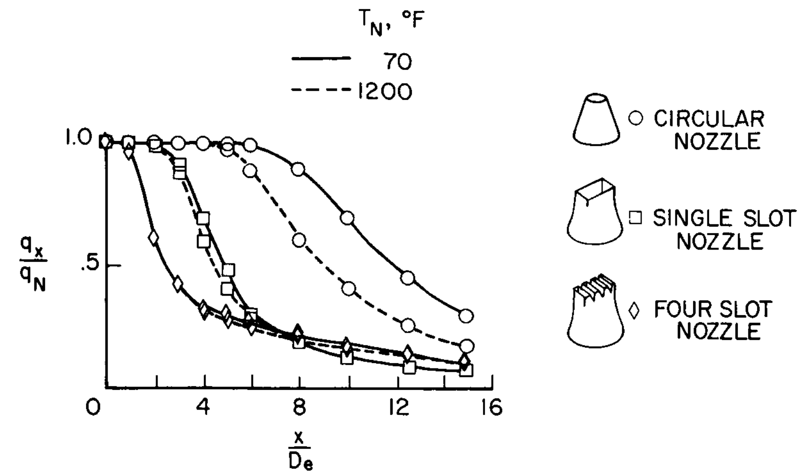

Figure 5.- Effect of nozzle configuration and temperature on jet decay.

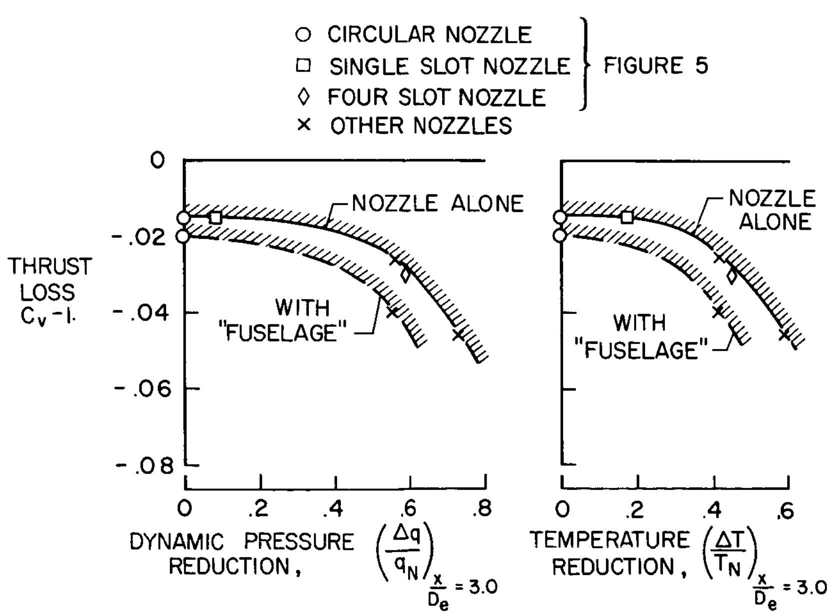

Figure 6.- Thrust loss and jet decay of suppressor nozzles.

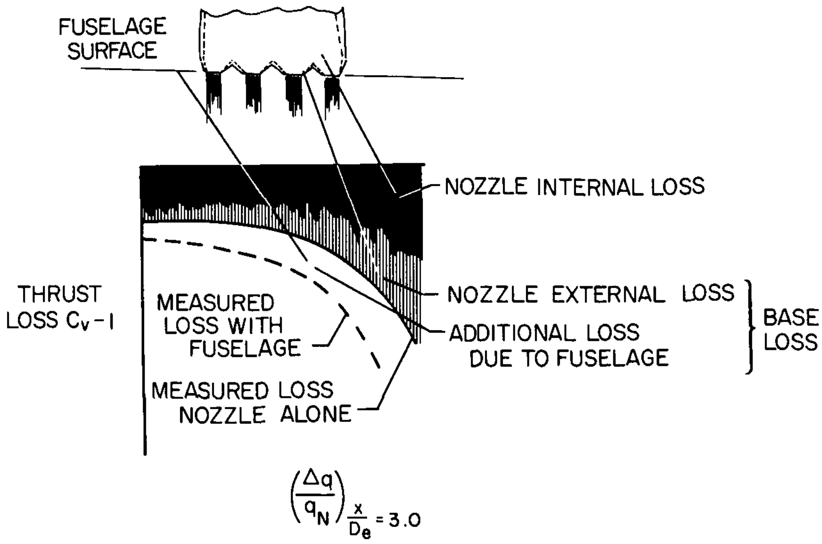

Figure 7.- Thrust losses on installed nozzles.

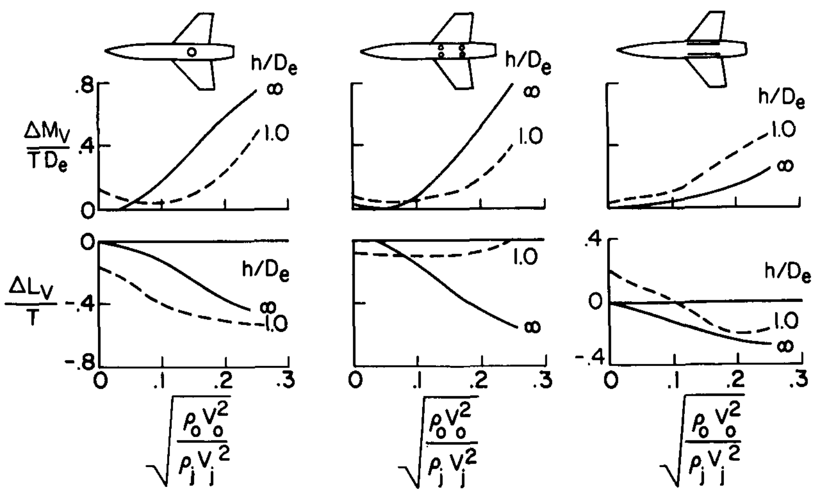

Figure 8.- Ground effect on jet interference in transition.

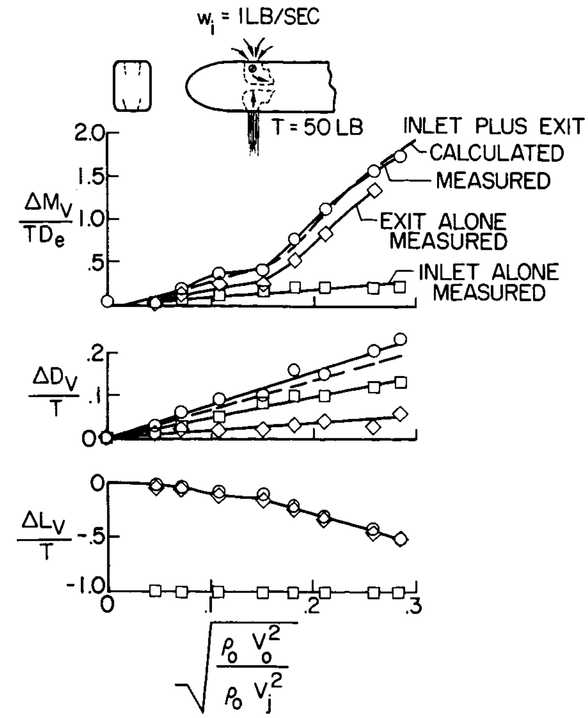

Figure 9.- Mutual interference of inlet and exit flows.

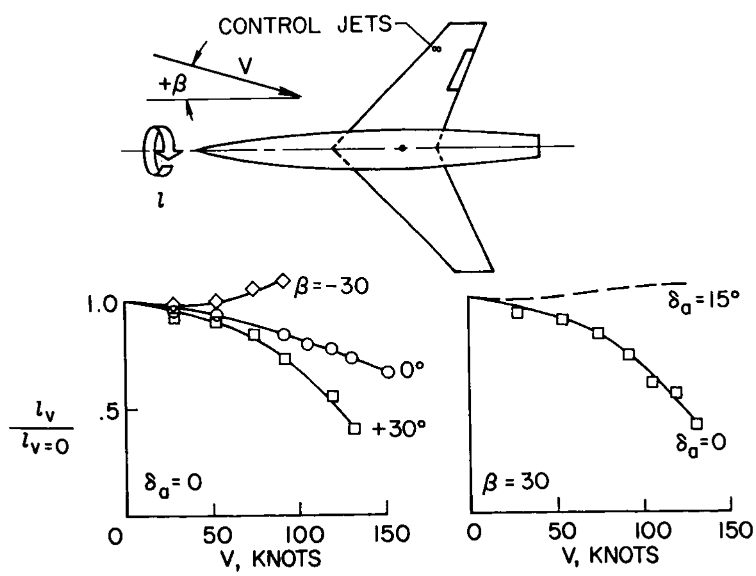

Figure 10.- Effect of velocity on roll control from tip jets.

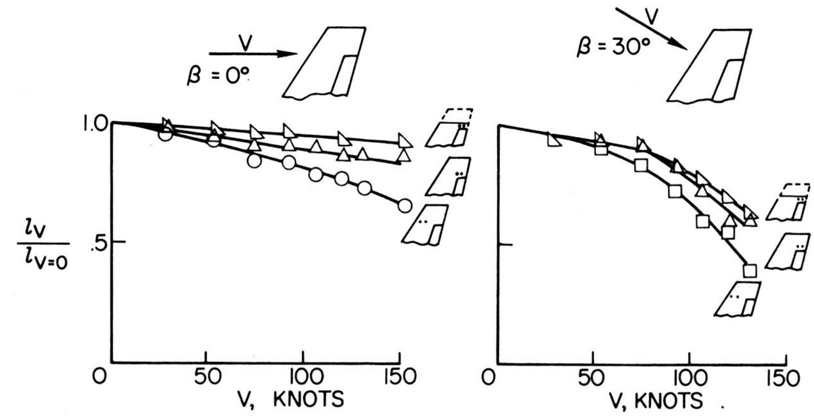

Figure 11.- Effect of jet location on roll control.

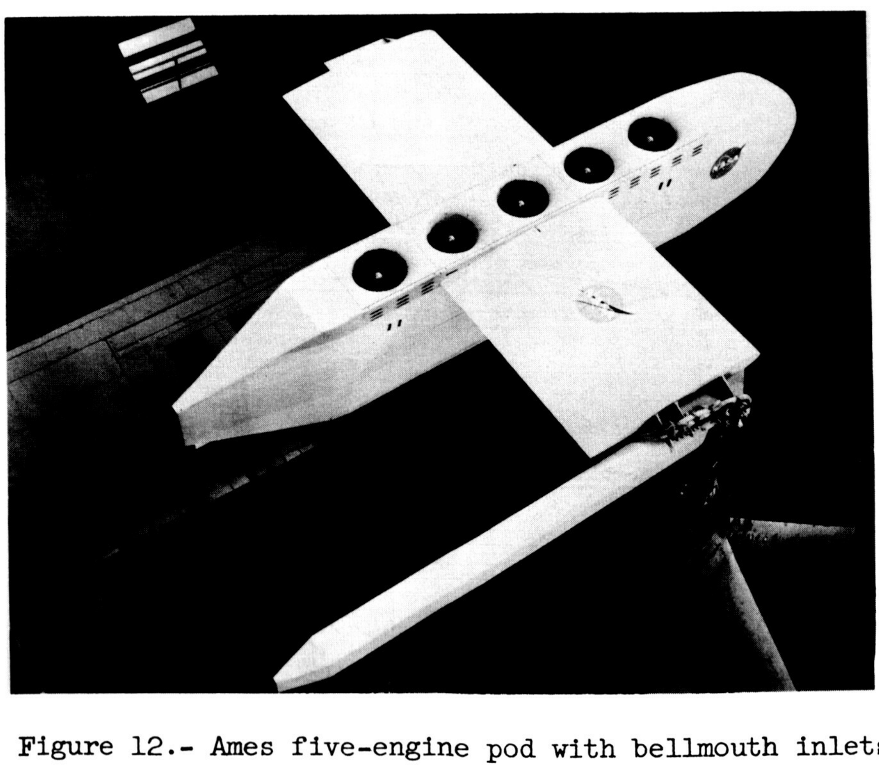

Figure 12.- Ames five-engine pod with bellmouth inlets.

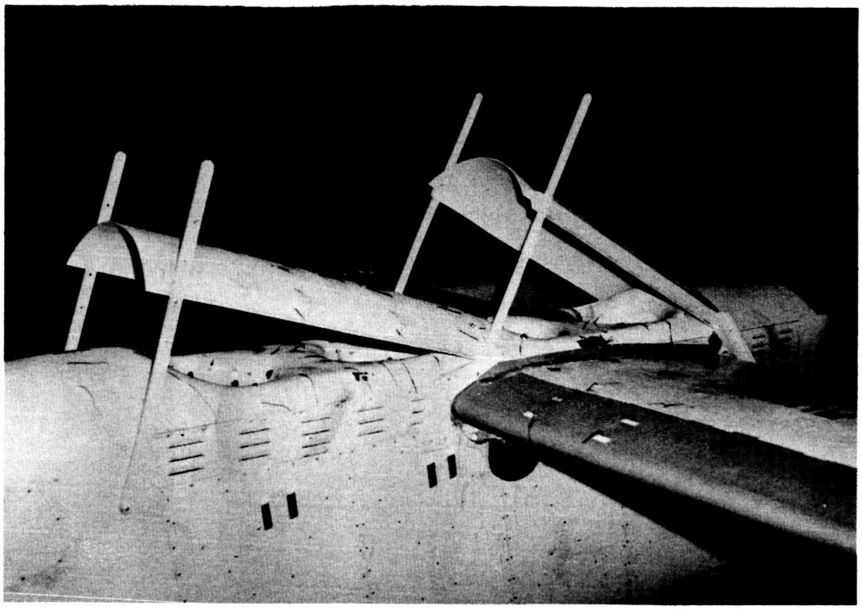

Figure 13.- Ames five-engine pod with scoop inlets.

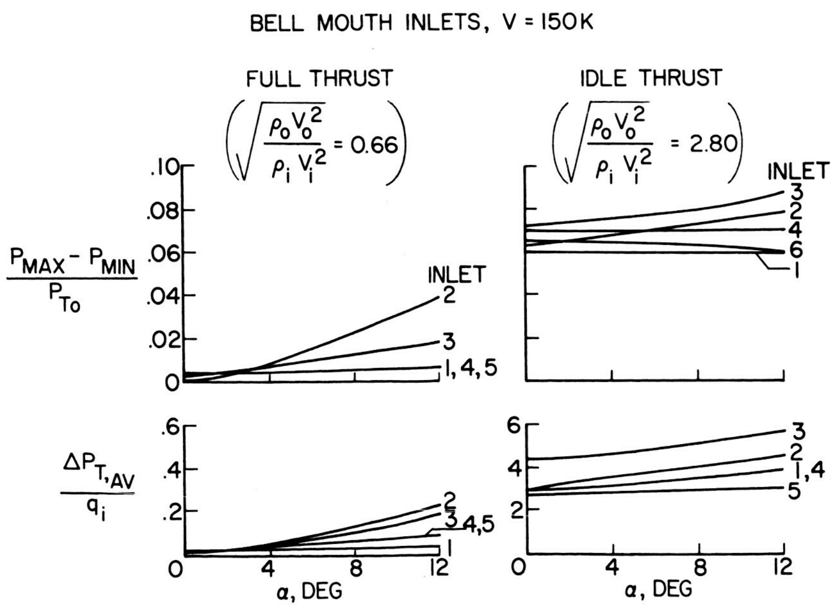

Figure 14.- Inlet distortion and pressure recovery.

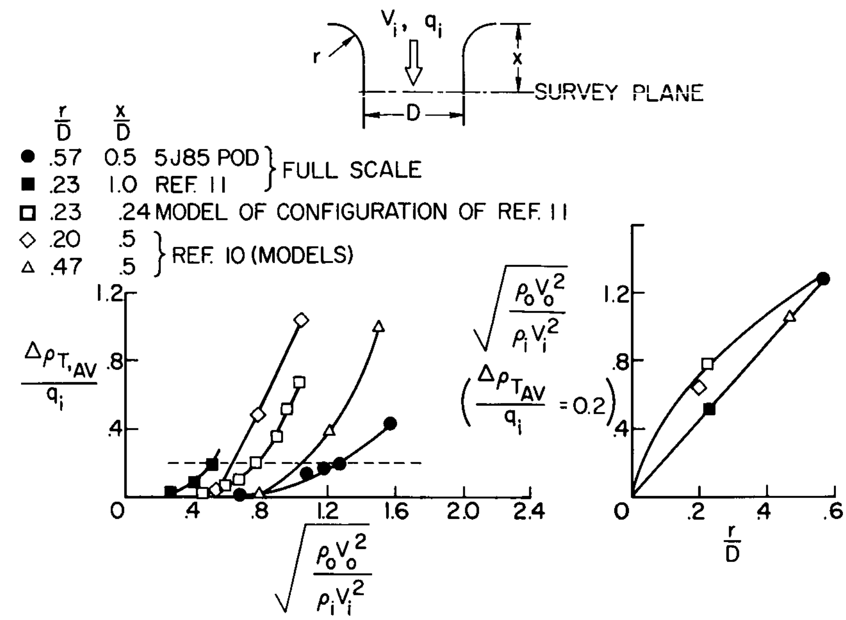

Figure 15.- Effect of inlet radius on pressure recovery.

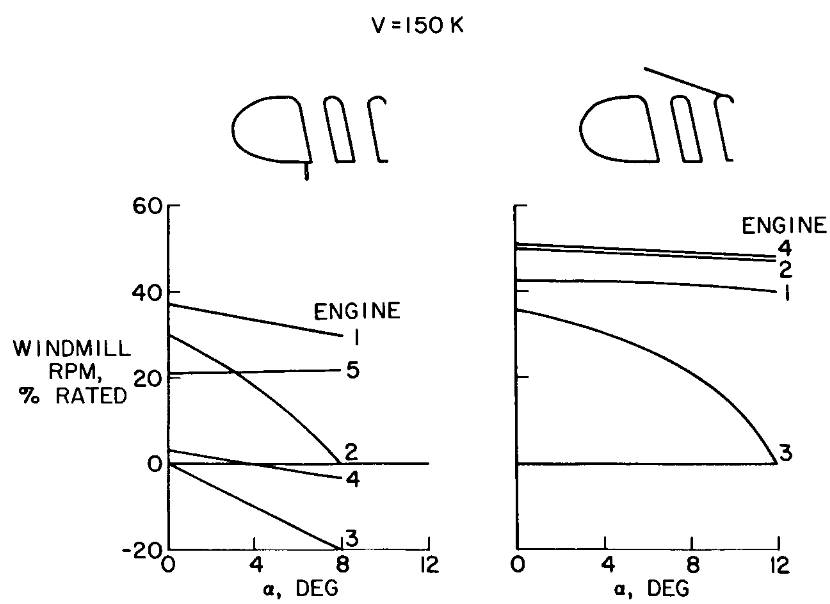

Figure 16.- Engine windmilling characteristics.

NASA-Langley, 1965